Chapter 1

Dominant-scale analysis for the automatic reduction of high-dimensional ODE systems

Robert Clewley
Center for Biodynamics, Boston University
rclewley@bu.edu

Near an orbit of interest in a dynamical system, it is typical to ask which variables dominate its structure at what times. What are its principal local degrees of freedom? How large is its basin of attraction? What bifurcations are nearby?

We describe a hybrid numerical and analytical technique that aids the identification of structure in orbits of a class of high-dimensional systems of ordinary differential equations. This 'dominant-scale' technique incorporates information about the separations in scale between variables, both in time and in a quantity we derive that measures a variable's *dominance strength* on an equation in which it appears. As such, the technique involves application of standard multiple-scale asymptotic analysis.

We demonstrate our technique using a new software tool, known as Dssrt, on a limit cycle of a regularly firing Hodgkin-Huxley neuron.

1.1 Introduction

Systems of ordinary differential equations (ODEs) arise commonly in the natural sciences as models of physical processes. Many of these models involve nonlinear dynamics [8], and exhibit complex behavior in a variety of ways. At the heart of much complex behavior lies the dynamics of variables working at different scales

of *time*. Furthermore, the form of interactions between the variables are often such that some do not have a significant effect over certain parts of the phase space. A common example is 'pulsatile' coupling [21], when a variable's input to another's equation only has an effect on the dynamics while the 'pulse' is occurring. This exemplifies multiple scales of *influence* in interactions between ODEs.

In many models studied using multiple-scale analysis it is common to find an *a priori* assumption of one or more explicit small parameters (e.g. the van der Pol [25], FitzHugh-Nagumo [7], Morris-LeCar [22] and Wilson-Cowan [27] oscillators, and weakly-coupled oscillators in general [10][17][21]). Typically these systems are amenable to a standard use of geometrical singular perturbation theory [4][11] and invariant manifold theory [6][26]. However, in other popular systems of equations, such as the Hodgkin-Huxley model of nerve action potential generation [9][14], we may instead find *more* than two time- or influence-scales (sometimes with a lack of strong separation), which may even swap their order of magnitudes during a typical oscillation [24]. Also, no explicit small parameter exists in the HH equations.

Techniques of dimension reduction exist in control theory and in dynamical systems modeling from the data analysis of time-series, and reduction methods for large chemical systems that focus on multiple scales in time with explicit small parameters [3][19]. Several *ad hoc* procedures exist in the modeling of neurophysiological rhythms [5][12], which is one of the primary motivations for this study. There is also a large body of literature focusing on the derivation of reduced neural models [1][7][15][16][18][20][27]. Here, we assume that an appropriate model for a particular analysis has already been decided.

We describe a 'dominant-scale' method of analysis for higher-dimensional models in which the separation of scales change through time, and where we take advantage of a measure of the influence that variables have on each other. We demonstrate our method's utility for a Hodgkin-Huxley type model of a single-compartment neuron that fires rhythmically (hereon abbreviated 'HH'). Our model is well known but has sufficient structure for us to briefly present the dominant-scale method and its analysis. As this model has been a popular subject of asymptotic analysis (e.g. [7][24]), this aids validation of—and intuition for—our method. Of course, our intention is to apply our methods to high-dimensional *coupled* systems, where intuition is less readily available and less reliable.Work in progress focuses on specific applications of this nature [23], and provides more detail and justification of the method and our derivations [2]. All calculations and graphics in this article originated from DSSRT (the *Dominant-Scale System Reduction Tool*), [1] a new software tool developed for use with Mathworks' MATLAB.

[1] The DSSRT software, with usage and technical documentation, full source code, and examples, is available at `http://math.bu.edu/people/rclewley/DSSRT.html`.

1.2 The Hodgkin-Huxley model

In order to efficiently introduce our method, it is useful to write the HH equations in unfamiliar notation. There is a current-balance equation for the membrane potential V. Associated equations for the dimensionless activation variables $g_x \in [0,1]$, where $x = m,\ h$, and n, model the 'spiking' excitability,

$$\begin{aligned} \tau_V\left(\{g_x\}_{x\in\Gamma_1}\right)\frac{\mathrm{d}V}{\mathrm{d}t} &= V_\infty\left(\{g_x\}_{x\in\Gamma_1\cup\Gamma_2}\right) - V \\ &= \bar{g}_m g_m^{\,3}\left(V_m - V\right) + \bar{g}_n g_n^{\,4}\left(V_n - V\right) \\ &\quad + \bar{g}_L g_L\left(V_L - V\right) + \bar{g}_I g_I \qquad (1.1) \\ \tau_x(V)\frac{\mathrm{d}g_x}{\mathrm{d}t} &= x_\infty(V) - g_x, \qquad x = m,\ h,\ n, \qquad (1.2) \end{aligned}$$

where the index sets are $\Gamma_1 = \{m, n, L\}$, and $\Gamma_2 = \{I\}$, and g_h is considered an auxiliary variable (see below). The voltage equation has the same form as for the activation variables, where we have defined

$$\begin{aligned} \tau_V &= C/\left(\bar{g}_m g_m^{\,3} + \bar{g}_n g_n^{\,4} + \bar{g}_L\right) \\ V_\infty &= \tau_V\left(\bar{g}_m g_m^{\,3} V_m + \bar{g}_n g_n^{\,4} V_n + \bar{g}_L V_L + \bar{g}_I g_I\right), \end{aligned}$$

and where we use $\bar{g}_n = 80$, $\bar{g}_L = 0.1$, $C = 1$, $V_m = 50$, $V_n = -100$, $V_L = -67$, $\bar{g}_I = 0.32$. For the 'leak' and 'drive current' inputs we have formally included the pseudo-gating *(passive)* variables $g_L(t) \equiv 1$ and $g_I(t) \equiv 1$, respectively. For the sodium activation current there are two gating variables, g_m and g_h, involved in forming the conductance. For our purposes (and without loss of generality) we treat g_m as the 'primary' variable, and have defined the maximal conductance $\bar{g}_m(t) = 100\ g_h(t)$. τ_x is a time-scale, and x_∞ is the 'asymptotic' value for x. We define $\tau_x = \alpha_x + \beta_x$ and $x_\infty = \frac{\alpha_x}{\alpha_x+\beta_x}$ in (1.2), using the forward and backward activation rates

$$\begin{aligned} \alpha_m(V) &= 0.32\,(V+54)\,/\left(1 - \mathrm{e}^{-(V+54)/4}\right) \\ \beta_m(V) &= 0.28\,(V+27)\,/\left(\mathrm{e}^{(V+27)/5-1}\right) \\ \alpha_h(V) &= 0.128\,\mathrm{e}^{-(50+V)/18} \\ \beta_h(V) &= 4.0\,/\left(1 + \mathrm{e}^{-(V+27)/5}\right) \\ \alpha_n(V) &= 0.032\,(V+52)\,/\left(1 - \mathrm{e}^{-(V+52)/5}\right) \\ \beta_n(V) &= 0.5\,\mathrm{e}^{-(57+V)/40}. \end{aligned}$$

The activation functions and parameters are typical for modeling mammalian cortical cells.

All the additive terms in the right hand side of the V equation (1.1) we refer to as *inputs*, because each term has a distinct physiological interpretation. There are two types of input: (a) additive 'current' terms, independent of V,

written $\bar{g}_x g_x^{q_x}(t)$ (index set Γ_1); (b) V-dependent 'conductance' terms of the form $\bar{g}_x g_x^{q_x}(t)\,(V_x - V)$ (set Γ_2). Here, $\bar{g}_x$ is the maximal value of the input, $g_x(t)$ is its time-course, and q_x is a positive integer.

1.3 Computing dominant inputs

We define the *dominance strength* of input term x to the V equation to be

$$\Psi_x(t) = g_x(t) \left| \frac{\partial V_\infty}{\partial g_x}(t) \right|, \quad x \in \Gamma_1 \cup \Gamma_2. \tag{1.3}$$

The factor of g_x normalizes the partial derivative. Because of the conditional linearity of the HH equations (i.e. each is linear in its own dependent variable if the other variable values are known), this definition reduces to a form that is computationally more practical, and which yields more insight into its meaning:

$$\Psi_x(t) = \begin{cases} \left| \frac{\bar{g}_x g_x^{q_x}(t)}{g_{tot}(t)} \left(V_x - V_\infty(t) \right) \right| & \text{if } x \in \Gamma_1, \\ \left| \frac{\bar{g}_x g_x^{q_x}(t)}{g_{tot}(t)} \right| & \text{if } x \in \Gamma_2. \end{cases} \tag{1.4}$$

We see that for Γ_1 inputs, Ψ_x resembles the input term for x except that V_∞ replaces V, and we have normalized by $g_{tot} \equiv 1/\tau_V$. This normalization occurred automatically from taking the derivative in (1.3), and has the benefit of allowing a fair comparison between Ψ_x values at times for which the effective membrane time constant τ_V differs greatly. For Γ_2 our definition coincides with the associated input term (modulo the normalizing factor). By defining a scale *relative* to the largest $\Psi_x(t)$ value, what is considered the $\mathcal{O}(1)$ dominant scale of influence is continually renormalized along an orbit.

Because there is only one input for each of the gating variable equations, we focus only on the V equation. All $\Psi_x(t)$ values associated with its inputs are calculated along any orbit $\tilde{\mathbf{X}}(t) \subset \mathbb{R}^4$, where $\tilde{\mathbf{X}} = (\tilde{V}, \tilde{g}_m, \tilde{g}_n, \tilde{g}_h)$ defines the coefficients of the orbit in each of the participating variables. At a sufficiently fine time resolution, the $|\Gamma_1 \cup \Gamma_2| = 4$ dominance strengths are ranked by size for each sample time t. In ratio form, each ranking can be expressed by the set of coefficients $c_i \in (0, 1]$ solving $\Psi_{x_i} = c_i \Psi_{x_1}$, where the coefficients define the scale of the i^{th} input relative to the strongest input x_1, and $\{x_i\}_{i=1\ldots4}$ is a permutation of $\Gamma_1 \cup \Gamma_2$. We do not have the convenience of an *explicit* small parameter in our system, so we introduce a free parameter $\varepsilon \in (0, 1)$, defining a small scale of influence between variables (typically not close to 0). Inputs having a scale coefficient $c_i > \varepsilon$ are called *active* inputs at time t, and form the ordered index set of actives $\mathcal{A}_{V,\varepsilon}(t)$. The remaining inputs are *inactive* at time t. ε must be set appropriately by the user for the method to be most effective. For instance, increasing ε forces DSSRT to be more exclusive, and produce simpler reduced models at the expense of accuracy.

1.4 Approximate local models

For all initial conditions, our HH system quickly approaches a limit cycle having period $T = 49.5$. Our method is independent of the orbit studied, but it is convenient to define $\tilde{\mathbf{X}}(t)$ to be this limit cycle hereon. The part of this cycle near a spike is shown in Fig. 1.1 for each of the constituent variables. We view the underlying structure of $\tilde{\mathbf{X}}(t)$ by recognizing a sequence of important events in the evolving dynamics. We define an *event* as occurring whenever there is a change in the set of all variables' actives $\bigcup_x \mathcal{A}_{x,\varepsilon}$, and we partition $\tilde{\mathbf{X}}(t)$ according to the times of these events. We define an *epoch* as the time interval between consecutive events. For a given ε, DSSRT partitions an orbit into $P(\varepsilon)$ epochs, having time intervals $\left[t_p, t_{p+1}\right)$ for $p = 1, \ldots, P-1$.

We use the definition of dominance strength to determine approximate local models to study the system near $\tilde{\mathbf{X}}(t)$, *independently* of the relative time-scales of the variables. We therefore assume an accurate knowledge of the time-courses of the variables making up $\tilde{\mathbf{X}}(t)$ (e.g. from numerical simulation). Within the p^{th} epoch, a suitable reduced model of the system *in a neighborhood* of $\tilde{\mathbf{X}}(t)$, for $t \in \left[t_p, t_{p+1}\right)$, is given by

$$\frac{\mathrm{d}V}{\mathrm{d}t} = \sum_{x\in\Gamma_1} \sigma_x \bar{g}_x g_x^{q_x} (V_x - V) + \sum_{x\in\Gamma_2} \sigma_x \bar{g}_x g_x^{q_x} \tag{1.5}$$

$$\frac{\mathrm{d}g_x}{\mathrm{d}t} = \frac{1}{\tau_x}(x_\infty - g_x), \qquad \text{if } \sigma_x = 1, \tag{1.6}$$

where the switch coefficients $\sigma_x(t) = 1$ if $x \in \mathcal{A}_{V,\varepsilon}(t)$ in this epoch, and zero otherwise. (Equations are absent for the passive inputs g_L and g_I.) The initial conditions are set to coincide with the corresponding entries of $\tilde{\mathbf{X}}(t_p)$. Each local model has an explicitly-estimated domain of validity (prescribed analytically and computed numerically), and is $\mathcal{O}(\varepsilon)$-accurate with respect to the full dynamics [2].

Using $\varepsilon = 1/3$ in DSSRT, we obtained a *transition sequence* of distinct $\mathcal{A}_{V,\varepsilon}$ sets associated with each of eight epochs. In Fig. 1.2, the set of computed epochs are overlaid on $\tilde{V}(t)$ for one period of the limit cycle, with the corresponding $V_\infty(t)$. An inset shows a close-up of these during a spike.

1.5 Reduced dynamical regimes

The sequence of local models was consolidated by DSSRT into four 'reduced dynamical regimes' using an algorithm that captures some of the essential intuition of matched asymptotic analysis for ODE initial-value problems. This requires tracking the changing orders of magnitude in the time-scales of active variables. For this we need a second free parameter, $\gamma \in (0, 1)$, that is a time-scale threshold for $\tau_x(t)/\tau_V(t)$ $(x \neq V)$. When this ratio is less than γ, then x is considered 'fast' relative to V. Here, active variables that are 'fast' are slaved to V, and their time-courses can be $\mathcal{O}(\gamma)$-approximated by their asymptotic value

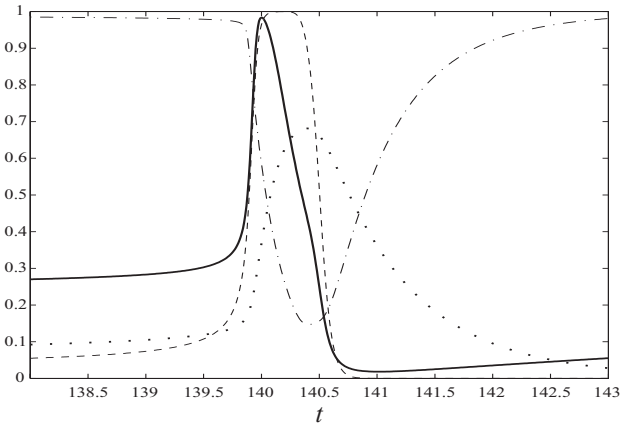

Figure 1.1: The four constituent variables making up $\tilde{\mathbf{X}}(t)$, focused on a spike. $\tilde{g}_m(t)$ is the dashed line, $\tilde{g}_n(t)$ is the dotted line, $\tilde{g}_h(t)$ is the dot-dash line, and for reference $\tilde{V}(t)$ is shown in bold, rescaled to $[0, 1]$.

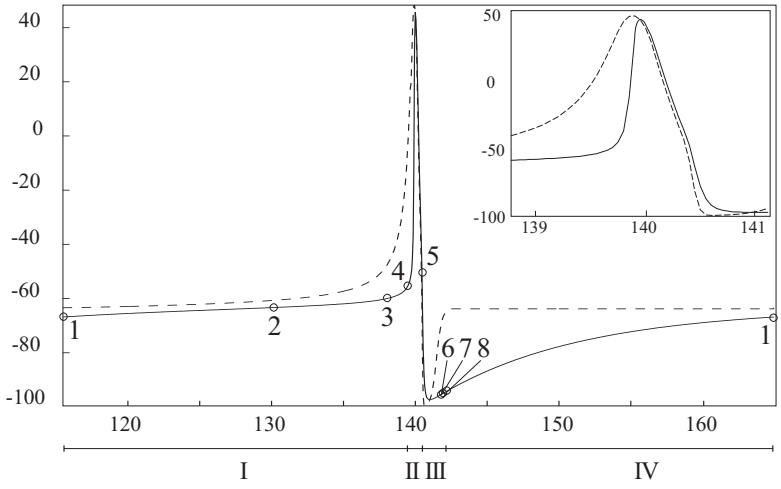

Figure 1.2: One period in $\tilde{V}(t)$, with $V_\infty(t)$, and its set of epochs. $V_\infty(t)$ is the dashed line. The epoch transition events are shown as open circles. The extent of each regime is marked below the time axis. The inset shows a close-up of the spike.

(an 'adiabatic elimination'), thereby reducing the model's number of dynamical variables further. Conversely, when the ratio is greater than $1/\gamma$ the variable is 'slow', and we can replace it in the regime with an appropriate constant value (determined self-consistently from looking at neighboring regimes). Here, we set $\gamma = 1/3$. Note the different focus of our method is that only the time-scales of the most dominantly influential (active) variables need to be considered; inactive variables are simply ignored in the local models.

I	$[115.45, 139.70)$	dim. = 2	**III**	$[140.65, 142.45)$	dim. = 1
Dynamic vars.		g_m[F], g_h, V	Dynamic vars.		g_n[F], V
Passive vars.		g_L, g_I	Passive vars.		g_L, g_I
Bifurcation param.		g_n	Bifurcation param.		
II	$[139.70, 140.65)$	dim. = 2	**IV**	$[142.45, 164.95)$	dim. = 1
Dynamic vars.		g_m, g_n[S], g_h[S], V	Dynamic vars.		V
Passive vars.			Passive vars.		g_L, g_I
Bifurcation param.			Bifurcation param.		g_m

Table 1.1: The four regimes determined by DSSRT: [F] indicates 'fast' variable, [S] indicates 'slow'. The half-open intervals mark the temporal extent of the regimes, and the effective dynamic dimension of each reduced model is also shown.

For instance, two epochs that differ only by passive variables are put in the same regime. The algorithm also attempts to determine which slowly changing or potentially active variables need to be tracked in order to accurately predict a transition into the next epoch.[2] Bifurcation analysis of the regimes can be done using these variables as quasi-static bifurcation parameters. Thus the regimes tell a concise story of the most important interactions between variables near orbits of interest in the full HH equations. Note that the construction of a trajectory near to $\tilde{\mathbf{X}}(t)$ using these regimes does not accumulate error through time because the HH system is strongly dissipative. Also, due to the emerging strong separation of dominance scale during a spike, the automatically generated regimes are not sensitive to changes in ε or γ.

The regimes calculated for the HH cell, shown in Table 1.1 and Fig. 1.2, show that the dynamics along most of the orbit is effectively one-dimensional, and only two-dimensional during a spike. Thus, standard graphical techniques can be used to do bifurcation analysis [8][10]. During a spike g_m, g_h and g_n play the most dominant roles (regimes I and II). These two regimes exactly correspond to those described in [24], where the phase-plane analysis of a cusp catastrophe and saddle-node bifurcation is detailed. The regimes also demonstrate the validity of a linear one-dimensional membrane model (e.g. the leaky integrate-and-fire model [18][13]) for the non-refractory part of the non-spiking dynamics, when only g_L and g_I are active inputs to the equation for V.

1.6 Summary and future work

With only minimal initial specification of the ODE system and the limit cycle to DSSRT, and selection of two free parameters, the software tool has resolved the important dynamical processes underlying an orbit of a HH model neuron—a 4-dimensional, stiff, and nonlinear ODE system involving pulsatile coupling between the variables, and changing time-scale relationships. It has generated a set of reduced dynamical regimes of low dimension within which bifurcation

[2] See online documentation and [2] for full details of the algorithms involved.

and perturbation analyses can be performed. In this simple example, the same regimes can be deduced by the application of standard multiple-scale analysis, using readily-available intuition (partly shown in [24]). This helps to validate our program's encoding of the intuition and analytical steps involved. Furthermore, major advantages of our method are the *quantitative* estimate of the domain of validity for each regime (both in time and with respect to perturbations from the limit cycle, without using numerical 'shooting' methods) [2], and the near-autonomy with which Dssrt establishes the regimes without needing formal small parameters. Dssrt can also deal with much larger and less familiar dynamical systems, where formal asymptotic analysis would be difficult by hand [23].

In future work we will use Dssrt to investigate the dynamical structure underlying the well-known phase-response curves for coupled oscillators, and add tools for automatic bifurcation analysis. We also hope to extend these methods to help more rigorously define and study concepts such as 'emergent structure' and 'self-organized complexity' in large dynamical systems. Certainly, a quantitative and computer-aided approach to formally reducing high-dimensional dynamical systems will be an important step towards achieving these goals.

Acknowledgements

Supported by NSF grant #DMS-0211505. Thanks go to Nancy Kopell, Horacio Rotstein and other members of the CBD for helpful comments and discussion.

Bibliography

[1] Abbott, Lawrence F., and T. B. Kepler, *Model neurons: from Hodgkin-Huxley to Hopfield*, vol. 368 of *Lecture notes in Physics*, Springer-Verlag, (1990), pp. 5–18.

[2] Clewley, Robert, "Dssrt: A computational tool for dominant-scale analysis of high-dimensional ODE systems", In preparation.

[3] Deuflhard, Peter, and J. Heroth, "Dynamic dimension reduction in ODE models", *Scientific Computing in Chemical Engineering*, (F. Keil, W. Mackens, H. Voss, and J. Werther eds.). Springer-Verlag (1996), pp. 29 – 43.

[4] Eckhaus, Wiktor, *Asymptotic analysis of singular perturbations*, North-Holland (1979).

[5] Ermentrout, G. Bard, and N. Kopell, "Fine structure of neural spiking and synchronization in the presence of conduction delays", *Proc. Nat. Acad. Sci. USA* **95** (1998), 1259–1264.

[6] Fenichel, Neil, "Persistence and smoothness of invariant manifolds for flows", *Ind. Univ. Math. J.* **21** (1971), 193–225.

[7] Fitzhugh, Richard, "Impulses and physiological states in models of nerve membrane", *Biophysical Journal* **1** (1961), 445–466.

[8] Guckenheimer, John, and P. Holmes, *Nonlinear Oscillations, Dynamical Systems, and Bifurcations of Vector Fields*, Springer-Verlag (1983).

[9] Hodgkin, Alan L., and A. F. Huxley, "Currents carried by sodium and potassium ions through the membrane of the giant axon of Loligo", *Journal of Physiology* **117** (1952), 500–544.

[10] Hoppensteadt, Frank C., and E. M. Izhikevich, *Weakly Coupled Neural Networks*, Springer (1997).

[11] Jones, Christopher K.R.T., "Geometric singular perturbation theory", *Dynamical systems, Montecatini Terme*, (L. Arnold ed.) vol. 1609 of *Lecture Notes in Mathematics*. Springer-Verlag (1994), pp. 44–118.

[12] Jones, Stephanie R., D. J. Pinto, T. J. Kaper, and N. Kopell, "Alpha-frequency rhythms desynchronize over long cortical distances: A modeling study", *J. Comp. Neurosci.* **9**, 3 (2000), 271–291.

[13] Keener, James P., F. C. Hoppensteadt, and J. Rinzel, "Integrate-and-fire models of nerve membrane response to oscillatory input", *SIAM J. Appl. Math.* **41**, 3 (1981), 503–517.

[14] Keener, James P., and J. Sneyd, *Mathematical Physiology*, Springer (1998).

[15] Kepler, Thomas B., L. F. Abbott, and E. Marder, "Reduction of conductance-based neuron models", *Biol. Cybern.* **66** (1992), 381–387.

[16] Kistler, Werner M., W. Gerstner, and J. L. van Hemmen, "Reduction of the Hodgkin-Huxley equations to a single-variable threshold model", *Neural Computation* **9** (1997), 1015–1045.

[17] Kopell, Nancy, and G. B. Ermentrout, "Symmetry and phaselocking in chains of weakly coupled oscillators", *Commun. Pure Appl. Math.* **39** (1986), 623–660.

[18] Lapique, L., "Recherches quantitatives sur l'excitation électriques des nerfs traitée comme une polarization", *J. Physiol. Pathol. Gen.* **9** (1907), 620–635.

[19] Maas, Ulrich, and S. B. Pope, "Simplifying chemical kinetics: Intrinsic lowdimensional manifolds in composition space", *Combustion and Flame* **88** (1992), 239–264.

[20] McKean, Henry P., "Nagumo's equation", *Advances in Mathematics* **4** (1970), 209–223.

[21] Mirollo, Rennie E., and S.H. Strogatz, "Synchronization of pulse-coupled biological oscillators", *SIAM J. Appl. Math.* **50** (1990), 1645–1662.

[22] Morris, C., and H. LeCar, "Voltage oscillations in the barnacle giant muscle fiber", *Biophysical Journal* **35** (1981), 193–213.

[23] Rotstein, Horacio, R. Clewley, and N. Kopell, "Multiple-scale analysis of a biophysical stellate cell model", In preparation.

[24] Suckley, Rebecca, and V.N. Biktashev, "Comparison of asymptotics of heart and nerve excitabilty", *Phys. Rev. E*, 011902 (2003).

[25] van der Pol, Balthazar, "Forced oscillations in a circuit with nonlinear resistance (receptance with reactive triode)", *Selected Papers on Mathematical Trends in Control Theory*, (R. Bellman and R. Kalaba eds.). Dover (1964).

[26] Wiggins, Stephen, *Normally hyperbolic invariant manifolds in dynamical systems*, Springer-Verlag (1994).

[27] Wilson, H. R., and J. D. Cowan, "A mathematical theory of the functional dynamics of cortical and thalamic nervous tissue", *Kybernetik* **13** (1973), 55–80.